Frontiers of Architectural Research (2013) 2, 468–475

Available online at www.sciencedirect.com

ScienceDirect

www.elsevier.com/locate/foar

Frontiers of Architectural Research

RESEARCH ARTICLE

Simulation-based feasibility study of improved air conditioning systems for hospital operating room

Zhiqiang (John) Zhai*, Anna L. Osborne

Department of Civil, Environmental, and Architectural Engineering, University of Colorado at Boulder, Boulder, CO 80309-0428, USA

Received 12 July 2013; received in revised form 11 September 2013; accepted 13 September 2013

KEYWORDS
Hospital operating room;
Air conditioning;
Computational fluid dynamics

Abstract
The goal of the air distribution inside a hospital operating room (OR) is to protect the patient and staff from cross-infection while maintaining occupant comfort and not affecting the facilitation of surgical tasks. In ORs, HEPA-filtered air and vertical (downward) laminar airflow are often used to achieve a unidirectional flow of fresh air from ceiling, washing over the patient and flowing out of exhaust vents on the side walls, near the floor. However, previous research has shown that this method does not necessarily achieve the desired unidirectional flow pattern or adequately achieve optimal air asepsis. The results from this study show that maximizing the area of the laminar flow diffusers remedies this issue and provides very low contamination levels. The use of air curtains as specified by manufacturers of commercial products may not provide satisfactory results, with noticeable contamination levels at the wound site.

1. Introduction

The goal of the air distribution inside a hospital operating room (OR) is to protect the patient and staff from cross-infection while maintaining occupant comfort and not affecting the facilitation of surgical tasks. However, a source of contamination bypasses HEPA installations in every OR, this source being the surgical staff themselves and the particles stirred up by their movement (Cook and Int-Hout, 2009). Therefore, air motion control must be used to maximize air asepsis.

In hospital ORs, using HEPA-filtered air and vertical (downward) laminar airflow is typical. ASHRAE Standard 170-2008 (ASHRAE, 2008) requires that ventilation be provided from the ceiling in a downward direction concentrated over the patient and surgical team. The area of the primary ventilation air diffusers must extend at least 305 mm beyond each side of the surgical table. It also requires that air is exhausted from

*Corresponding author. Tel.: +1 303 492 4699.
E-mail address: John.zhai@colorado.edu (Z. Zhai).
Peer review under responsibility of Southeast University.

Production and hosting by Elsevier

http://dx.doi.org/10.1016/j.foar.2013.09.003

at least two grilles on opposing sides of the room near the floor. It requires the use of non-aspirating, Group E outlets that provide a unidirectional flow pattern in the room (aka laminar flow diffusers). However, previous research has shown that this method does not necessarily achieve the desired unidirectional flow pattern or adequately achieve optimal air asepsis (Zhai et al., 2013). Zhai et al. (2013) used on-site field experiment, full-scale laboratory experiment, and computational modeling to verify and test the current ventilation practices in OR. Both experimental and simulation results showed a strong inward contraction of the supply air jet, instead of a unidirectional downward flow. The buoyancy forces on the downward supply air jet were determined to be the cause of the observed air distribution pattern.

This research will build upon the study of Zhai et al. (2013) by testing alternative air supply configurations which may maximize air asepsis. The pattern of the airflow will also be studied to determine if it provides a more unidirectional airflow.

2. Computer model setup

A computational fluid dynamics (CFD) tool was used to predict the flow pattern and contaminant transport in a representative OR environment. CFD has been widely used in indoor environment study (Spengler and Chen, 2000; Chen and Zhai, 2004; Zhai et al., 2007 etc.). A same CFD model as that used in Zhai et al. (2013) was rebuilt by this study and validated against the full-scale laboratory experiments. The same diffuser specifications and air change rate per hour (ACH) as tested in the experiment were used in the initial CFD model, as well as the same room and equipment and occupant conditions, as shown in Table 1 and Figure 1. These objects and heat gain values were chosen based on detailed on-site OR studies and measurements (Zhai et al., 2013). The equipment thermal loads as well as temperature of the patient's wound and skin can be seen in Table 2. Table 3 indicates the sizes of all of the objects in the room.

3. Computer model validation

3.1. Grid independence

The results of a CFD simulation are highly dependent on the quality of the computational grid. Based on the suggestion of Zhai et al. (2013), a grid refinement study was conducted on the three grids: $70 \times 58 \times 45$ (183,000 cells), $87 \times 73 \times 57$ (362,000 cells), and $106 \times 91 \times 70$ (675, 000 cells). Figure 2 demonstrates the finest grid distribution.

Table 1 Laboratory experiment specifications.

Room dimensions	$6.1 \times 5.8 \times 2.9$ m^3
Diffuser dimensions	2.44×3.05 m^2
Diffuser coverage area	7.06 m^2
Air change rate	31.6
Nominal face velocity	0.127 m^3/s m^2
Room air temperature	20 °C
Supply air temperature	18.3 °C
Room pressurization	+2.5 Pa

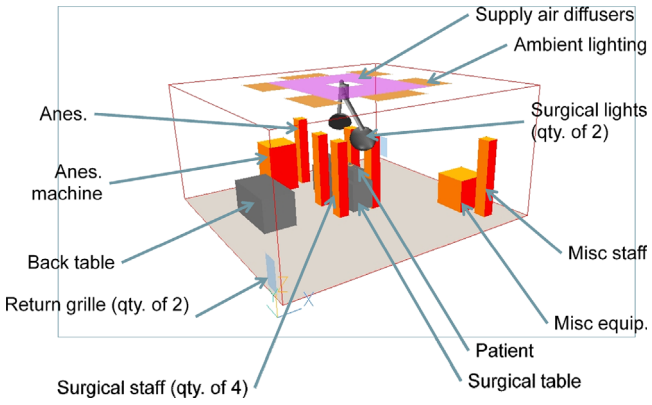

Figure 1 Base CFD model setup.

Table 2 Laboratory thermal loads.

Object	Qty	Heat gain (W)	Temperature (°C)
Manikins - male	2	80	
Manikins - female	4	68	
Anesthesia machine	1	100	
Surgical lights	2	250	
Monitor	1	200	
Ambient lights	6	128	
Patient wound	1		25.6
Patient skin	2		27.4

Table 3 Room object dimensions.

Object	Qty	Dimensions (m)
Surgical table	1	$0.54 \times 1.88 \times 0.66$
Back table	1	$0.76 \times 1.52 \times 0.76$
Anesthesia machine	1	$0.76 \times 0.76 \times 1.2$
Surgical lighting	2	0.58 diameter
Misc. equipment (Monitor)	1	$0.76 \times 0.76 \times 0.76$
Surgical staff	6	$0.25 \times 0.30 \times 1.75$
Patient body	1	$0.30 \times 1.60 \times 0.25$

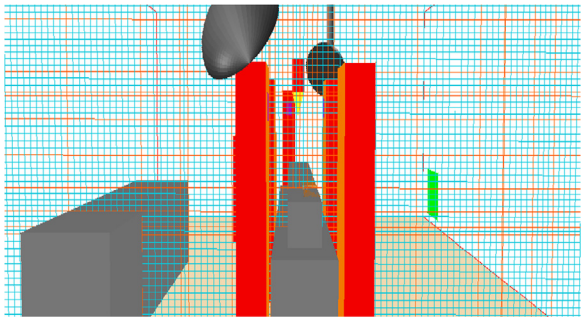

Figure 2 Grid refinement case: 675 K cells.

These grids were evaluated using the normalized root mean squared error (NRMSE) of the CFD model results with different grids. Figure 4 shows the NRMSE of the predicted U and W direction velocity at the four measure poles (1–4) across the center axis of the room (2.88 m) (shown in Figure 3), between the 180 and 362 K meshes and the 675 K mesh. It reveals that there is generally a great improvement in error with the 362 K mesh, and the computational error is typically below 10%, and absolutely below 30%. Based on these, and in order to minimize the simulation time, the 362 K mesh was chosen to be used for the parametric simulations.

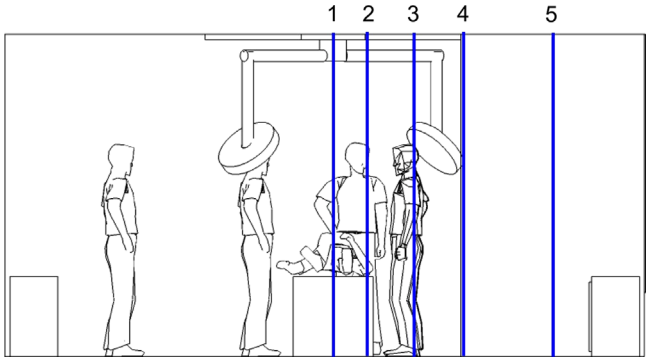

Figure 3 CFD grid refinement measurement locations in central cross-sectional plane (1. Center of room; 2. Interior edge of diffuser; 3. Midpoint of diffuser; 4. Exterior edge of diffuser; 5. Midpoint of outer region of room).

3.2. Comparison with experiments

The study replicates the airflow pattern as observed by Zhai et al. (2013): an inward curvature of the airflow to the center of the jet stream, as seen in Figure 5. This behavior reduces the overall coverage area and could pose a contamination risk to the patient.

The quantitative comparisons of simulation and experimental results were plotted in Figures 6 and 7, for U (X) and W (Z) velocity component, respectively. Figures 6 and 7 show that the CFD simulations closely follow the experimental results, with a few exceptions. It also appears that there is, in general, a large difference between the experimental results and the 180 K mesh, but a smaller difference between the 362 and 675 K meshes.

4. Air distribution simulation with improved air conditioning systems

To avoid the in-ward flow under the unidirectional diffuser, a few practical strategies were tested using the validated CFD model. The first was to create vertical downward air curtain around the laminar diffuser. Several commercial products are

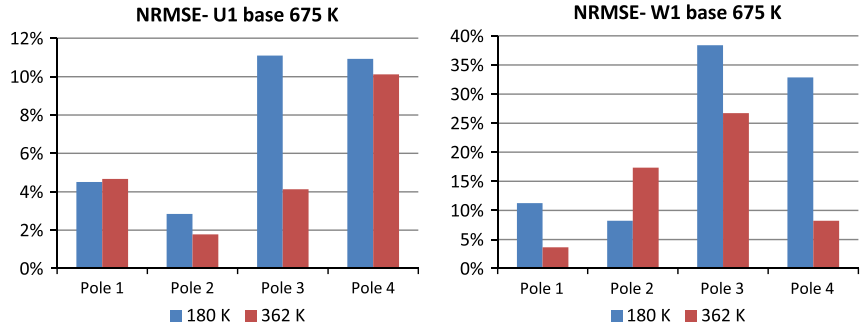

Figure 4 NRMSE comparison between 180 K and 362 K meshes and 675 K mesh.

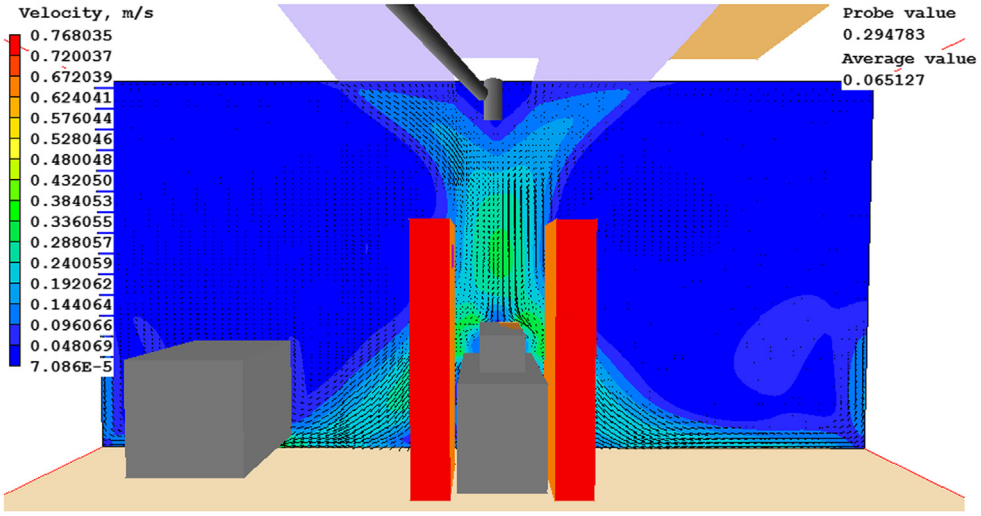

Figure 5 Velocity vectors and contours at the central cross section with 675 K grid.

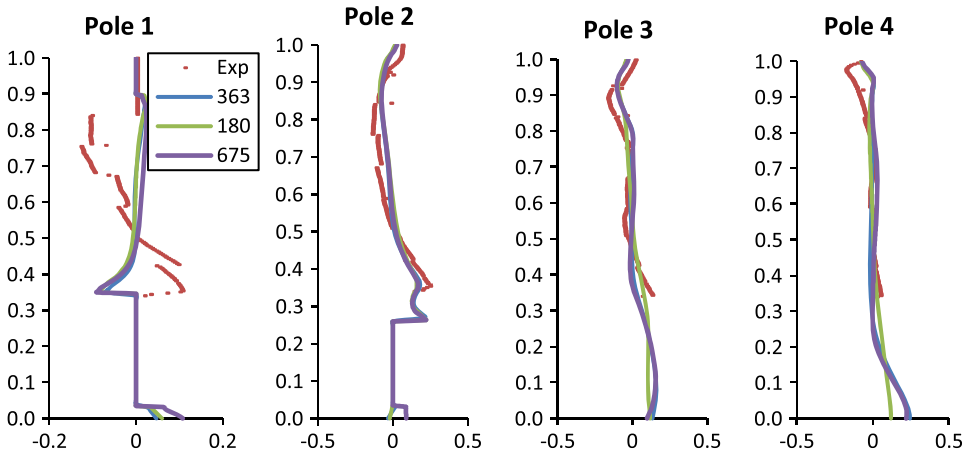

Figure 6 Comparison of *U*-velocity in the *X* direction.

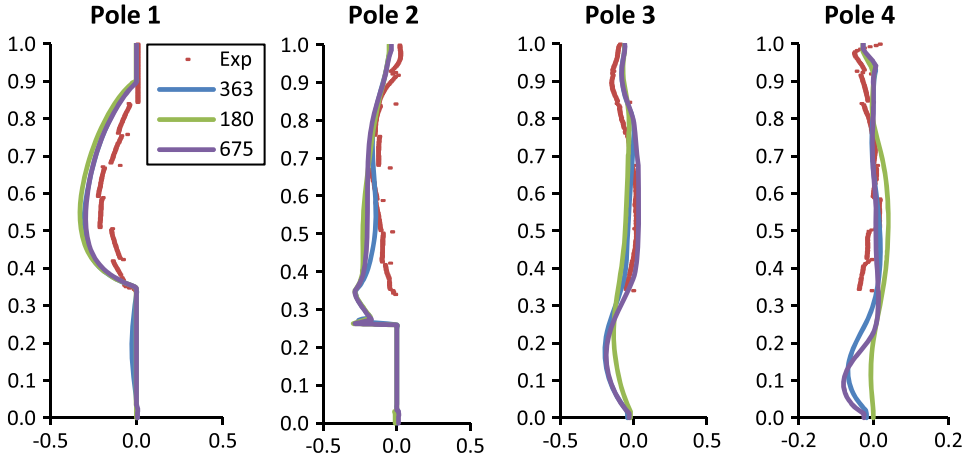

Figure 7 Comparison of *W*-velocity in the *Z* direction.

available which create an "air curtain" barrier between the operating area and the rest of the room, as illustrated in Figure 8. The system attempts to create a physical barrier that separates the surgical area from the recirculating air in the perimeter of the room while directing particulates toward exhaust grilles. This system uses three main components, the laminar flow diffuser, the linear slot diffusers (or "air curtains"), and low-level exhaust grilles. Four air curtain cases were thus created, three followed the manufacturer design specifications, and one did not. The fifth case simply tested the effects of a larger area of laminar flow diffusers without using air curtain.

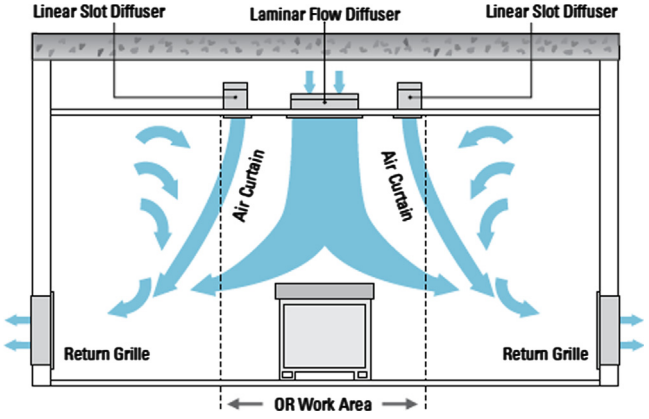

Figure 8 Diagram of a typical air curtain system.

4.1. Cases 1-3: air curtain design cases

A typical air curtain system was modeled according to the design specifications (Price Industries Limited, 2011). This includes a minimum contained area at the size of the operating table plus 3 ft (915 mm) perimeter work area, and a minimum of 20 ACH as recommended by ASHRAE. To develop a proper air curtain, the system must have a minimum recommended air flow of 30 cfm per linear foot (46 L/s per linear meter) and a maximum of 40 cfm/lf (62 L/s per linear meter). The air curtain should be selected to supply 60-75% of the total air supply into the operating room. Therefore, the laminar flow diffusers (LFD) must supply 25-40% of the total operating room air. The LFD are located within the perimeter of the air curtain, at a minimum of 1 ft (0.3048 m) from any linear slot diffuser to avoid entrainment of the laminar flow into the air curtain. ASHRAE Standard 170-2008 (ASHRAE, 2008) defines the primary

diffuser area (PDA) as the ceiling area directly above the operating table plus a 1 ft (0.3048 m) offset on all sides. All cases were based on 40% of total room supply air flow rate provided by the LFD and 60% of air provided by the air curtain. The system was sized starting with the PDA as described in Table 4. Based on this area, panels were selected from the literature (Price Industries Limited, 2011). Next, the operational volumetric flow rate of the panel was selected. For Cases 1 and 2, only the available cfm as described in the LFD Series Performance Data was used (120 and 80 cfm, respectively) (Price Industries Limited, 2011). For Case 3, 100 cfm was used, resulting in the same face velocity as the original model by Zhai et al. (2013).

Table 4 Primary diffuser area.

Length of surgical table	1.88 m
Width of surgical table	0.54 m
Area of surgical table	1.02 m^2
Length of PDA	2.49 m
Width of PDA	1.15 m
PDA	2.86 m^2

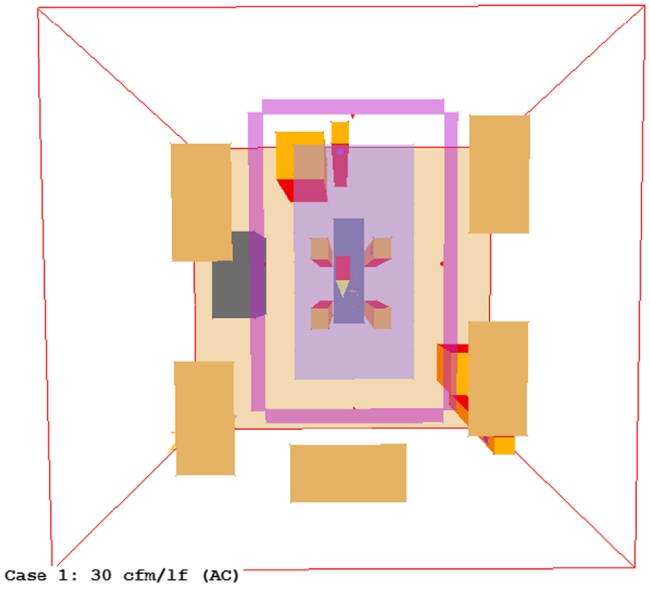

Figure 9 Cases 2 and 3 CFD setup (top view).

Next, the total room cfm was calculated based on a supply ratio of 40% for the LFD. The ACH was calculated using

$$\text{Air change rate per hour} = \frac{\text{Total room cfm} \times 60\ \text{min/h}}{\text{Volume of room}} \quad (1)$$

The air curtain cfm was calculated based on the LFD cfm and the total room cfm, which are known. Then, ensuring that the air curtain is at least 1 ft (0.3048 m) from the LFD, the length and width were selected and the flow rate per linear meter was calculated based on the required cfm and the number of linear meters. This was done while checking that the flow rate per linear meter stayed within the recommended boundaries (46–62 L/s lm). The used LFD has a free area of 13%, and the tested air curtains have a free area of 33%. The air curtains deliver air at 15° from vertical away from the work area. All of these specifications were accounted for in the CFD model (Table 5). Figure 9 shows the setup of Cases 2 and 3.

4.2. Case 4: alternative air curtain setup

Case 4 tested an air curtain that was located just around the operating table, between the patient and the surgical staff. Laminar flow diffusers were located inside and outside the curtain. This system did not follow the manufacturer specifications. Table 6 presents the air distribution specifications and Figure 10 illustrates the corresponding CFD model.

4.3. Case 5: larger laminar flow diffuser

The final case tested the effects of a larger area of laminar flow diffusers. The base case had a gross diffuser area of 7.06 m^2. This case has a net area of 7.46 m^2. Table 7 presents the corresponding air distribution specifications.

Table 5 Air distribution specifications.

	Case 1	Case 2	Case 3
LFD dimensions	0.305 m × 1.219 m		
Number of LFD	8		
Total LFD area	2.97 m^2		
Flow rate per LFD	56.63 L/s	37.76 L/s	47.19 L/s
LFD face velocity	0.1524 $m^3/s\ m^2$	0.1016 $m^3/s\ m^2$	0.127 $m^3/s\ m^2$
Total LFD, L/s	453	302	377.6
Total room, L/s	1132.7	755.1	943.9
Total room ACH	39.81	26.54	33.18
Total air curtain (AC), L/s	679.6	453.1	566.3
AC length	3.66 m	3.05 m	3.05 m
AC width	1.83 m	1.83 m	1.83 m
Flow rate per linear meter	61.94 L/s lm	46.45 L/s lm	58.06 L/s lm
AC face velocity	1.22 $m^3/s\ m^2$	0.91 $m^3/s\ m^2$	1.14 $m^3/s\ m^2$

Table 6 Alternative air distribution specifications.

Total LFD area	2.59 m^2
Flow rate per LFD	66.07 L/s
LFD face velocity	0.127 $m^3/s\ m^2$
Total LFD, L/s	330.4
Total room, L/s	825.9
Total room ACH	29.03
Total air curtain, L/s	495.5
AC length	3.05 m
AC width	1.83 m
Flow rate per linear meter	46.45 L/s lm
AC face velocity	0.91 $m^3/s\ m^2$

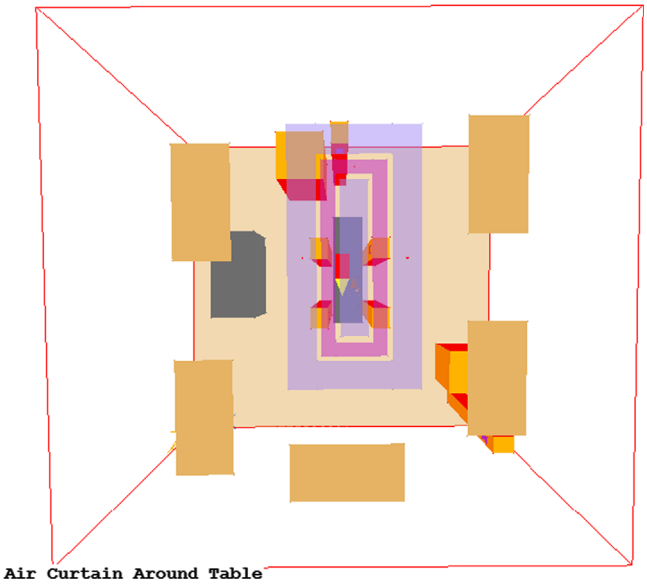

Figure 10 Case 4 CFD setup (top view).

Table 7 LFD case specifications.

LFD dimensions	2.43 m × 3.07 m
Total LFD area	7.46 m^2
Flow rate per LFD	56.63 L/s
LFD face velocity	0.127 $m^3/s\ m^2$
Total LFD, L/s	947.4
Total room ACH	33.3

5. Particle transport simulation with improved air conditioning systems

Indoor contaminants were tracked by releasing a generic but distinguished contaminant (C1–C4), respectively, from four of the surgical staff, at a concentration of 1000 ppm. The concentrations of these particles in the air just above the wound site and at the edge of the back table were measured in CFD. This method was used to determine the overall effectiveness of each diffuser setup. The particles were released from 0.1 m × 0.15 m plates located at 1.45 m off the ground on the surface of staff members 1–4 as shown in Figure 11. This included two staff members directly next to the patient, and two staff members on the perimeter of the OR.

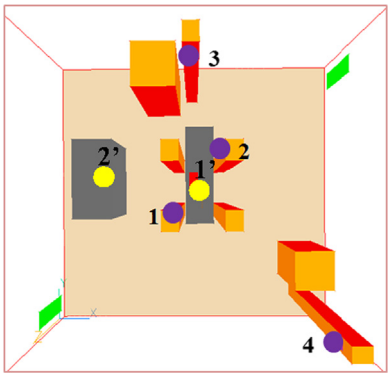

Figure 11 Locations of particle release (1: 2.85, 2.45, 1.45; 2: 3.49, 3.45, 1.45; 3: 2.98, 4.99, 1.45; 4: 5.24, 0.56, 1.45) and measurements (1′: 3.24, 2.81, 1.01; 2′: 1.40, 3.10, 0.76) (unit: m).

Table 8 Contamination levels at the wound site.

	C1	C2	C3	C4	Avg
Baseline model (362 K)	0.018	0.0008	0.0045	0.045	0.017
Baseline model (675 K)	0.033	0.0008	0.0083	0.052	0.024
AC model case 1	1.41	2.17	0.78	2.06	1.605
AC model case 2	3.41	2.08	0.082	1.05	1.656
AC model case 3	2.47	1.23	0.63	2.45	3.108
AC model case 4	1.91	0.66	0.02	1.72	1.078
LFD model case 5	0.084	0.0	0.0	0.0002	0.021

6. Simulation results and discussion

All five cases were run in a commercial CFD program for a total of 5000 iterations using a mesh size of 362 K. All of these cases also included the contamination sources as described in the "Particle Transport" section. The concentration level in the air at the wound site and on the middle edge of the back table was measured, and these results can be seen in Tables 8 and 9.

The baseline models had relatively low contamination levels, both at the wound site and at the back table. Cases 1–3, which followed the specifications, had the highest contamination levels, ranging from 0.082 to 3.41 at the wound site, and 0.31 to 10.1 at the back table. Case 1 had the highest LFD and air curtain flow rates. It had a lower contamination level from the staff member directly next to the wound (Source 1) than the other two cases, but the highest contamination level from Source 2. Of the three cases, Case 2 had the lowest LFD and air curtain flow rates. It has the lowest contamination level at the wound site from Source 3, but the highest contamination level from Source 1. Case 3 had an in-between LFD and air curtain flow rate, and resulted in the highest contamination from Sources 3 and 4.

For the back table, all three cases were much closer in concentration for all sources, with the exception of Source 3. This source resulted in a very high concentration for Case 1 and a lower concentration for Case 3. Based on average concentration levels for all four sources, Case 2 yielded the best results out of the three models.

Case 4 uses similar LFD and air curtain flow rates as Case 2. It performed better than Case 3 at both the wound site and the back table, and performed better than Case 1 at the back table. Case 5 was by far the best performance. It had lower average concentrations than the baseline cases. Figures 12-14 present the predicted velocity patterns for Cases 1, 4 and 5. Cases 2 and 3 have similar flow patterns as Case 1.

Table 9 Contamination levels at the back table.

	C1	C2	C3	C4	Avg
Baseline model (362 K)	0.037	0.0095	0.091	0.0084	0.036
Baseline model (675 K)	0.11	0.033	0.82	0.018	0.245
AC model case 1	1.88	0.80	10.1	0.50	3.320
AC model case 2	1.91	0.33	0.39	0.39	0.755
AC model case 3	2.19	0.51	4.03	0.31	1.760
AC model case 4	1.92	2.42	0.35	0.42	1.278
LFD model case 5	0.00005	0.0073	0.0012	0.0	0.002

7. Conclusions

This paper describes some recent excises on evaluating the feasibility of improving air conditions in hospital ORs. The results do not show a clear correlation between LFD and air curtain flow rates and concentration. However, they do

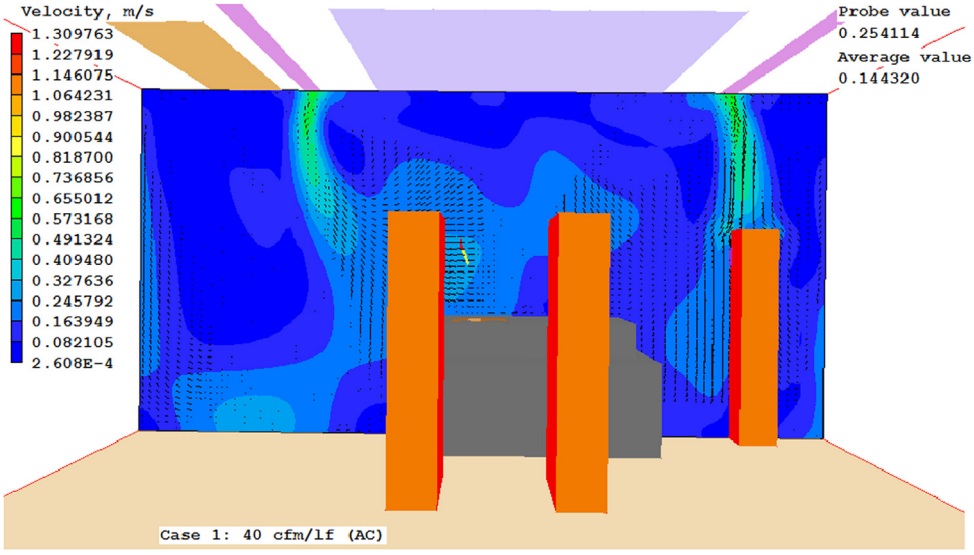

Figure 12 Case 1 velocity at cross section.

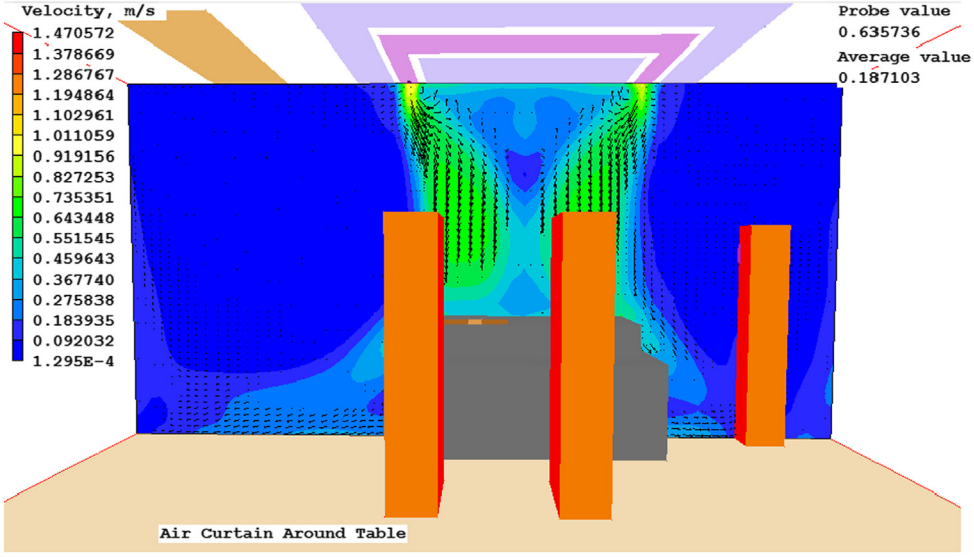

Figure 13 Case 4 velocity at cross section.

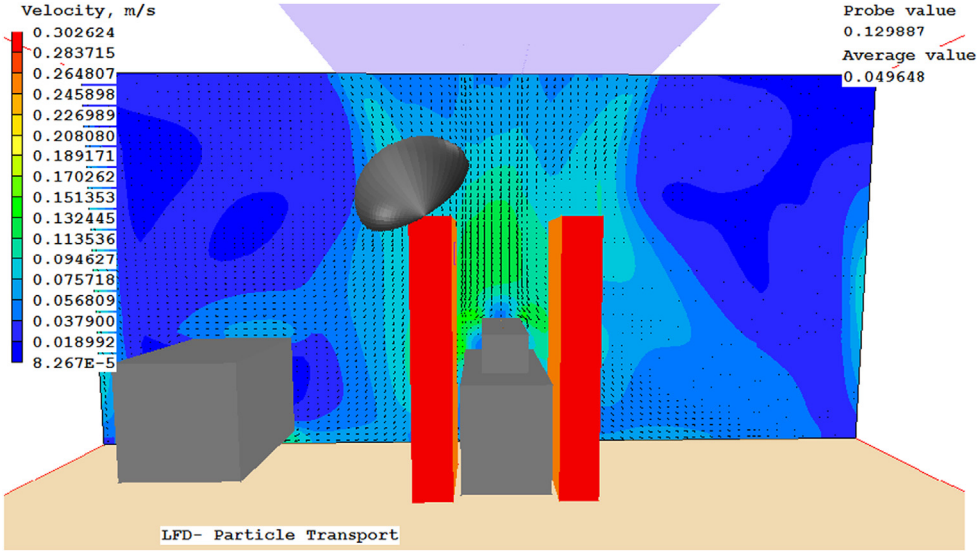

Figure 14 Case 5 velocity at the cross section.

show that following the specifications for sizing the air curtain and laminar flow diffusers may not necessarily result in a better indoor environment than the baseline model. This difference could be attributed to the coverage area of the LFD. The baseline model has 7.06 m^2, while the air curtain models only have 2.97 m^2. The unidirectional flow provided by these LFDs seems a much better method of achieving maximum air asepsis than using a high velocity air curtain. This theory is reinforced by the results of Case 5, which by far yields the best results, with almost no contamination at the wound or on the back table. Expansion on this work could include adding more laminar flow diffusers outside of the air curtains to see if performance is improved.

References

ASHRAE, 2008. ANSI/ASHRAE Standard 170-2008. Ventilation of Healthcare Facilities. American Society of Heating, Refrigerating, and Air-Conditioning Engineers, Inc., Atlanta.

Chen, Q., Zhai, Z., 2004. The use of cfd tools for indoor environmental design. In: Malkawi, A., Augenbroe, G. (Eds.), Advanced Building Simulation. Spon Press, New York, pp. 119–140.

Cook, G., Int-Hout, D., 2009. Air motion control in the hospital operating room. ASHRAE Transactions 51 (3), 30–36.

Price Industries Limited, 2011. Price OR Systems: Air Curtain System.

Spengler, J.D., Chen, Q., 2000. Indoor air quality factors in designing a healthy building. Annual Review of Energy and the Environment 25, 567–600.

Zhai, Z., Zhang, Z., Zhang, W., Chen, Q., 2007. Evaluation of various turbulence models in predicting airflow and turbulence in enclosed environments by CFD: Part-1: summary of prevent turbulence models. HVAC&R Research 13, 6.

Zhai Z, McNeill J. Hertzberg J. Experimental investigation of hospital operating room (OR) air distribution (TRP-1397). Final Report to American Society of Heating, Refrigerating, and Air-Conditioning Engineers, Inc., Atlanta, 158 pages, 2013.